Characterization of ARIES/SDI Periodic Noise

1 Summary of ARIES SDI observations – darks and sky frames

15 October 2003 – darks, sky frames, and a few frames of GJ 799AB acquired.

12 February 2004 – Partial datasets acquired for V577 Per A and V834 Tau. Not science quality due to poor seeing. Darks and sky frames acquired.

5-6 May 2004 – Full dataset acquired for DX Leo. Darks and sky frames acquired.

25 April 2005 – Darks and sky frames acquired at end of night.

26 April 2005 – Two datasets acquired, only one is reasonable quality. Darks and sky frames acquired.

30 April 2005 - 1 May 2005 – Good quality datasets acquired for 7 stars. Darks and sky frames acquired.

2 ARIES Periodic Noise Characteristics

A periodic noise pattern appears in nearly every sky, dark, and data frame from the ARIES SDI device. Often, multiple periodicities and beating are evident. Noise amplitudes (peak to trough) vary from $\sim$1 adu to $\sim$10 adu. Noise wavelengths range from $\sim$1 to $\sim$10 pixels. The angle of the noise pattern appears to be random and varies over the course observations. The noise properties often change rapidly, sometimes on minute to minute timescales.

2.1 Data processing

For the purpose of noise analysis, all skys and darks underwent the same basic data processing:

1) standard crosstalk correction: corquad script in IRAF

2) bad pixels removed using crmedian task in IRAF

4) shade pattern removed from image using IDL script rm_shade.pro. This script simply subtracts the median value of each row in the image from each pixel in that row.

5) The image was smoothed using a 10σ Gaussian and then the smoothed image was subtracted from the original image to remove low spatial frequencies and approximate flat-fielding.

6) To isolate the periodic noise component from the high-spatial frequency read noise, the image was smoothed with a 0.5σ Gaussian.

Sample processed images appear in Fig. 1.

2.2 Sample images from the night of May 1, 2005

Two consecutive 30 s sky frames (after standard data processing as described above) are presented in Fig. 1. In both frames, a strong periodic noise component is immediately

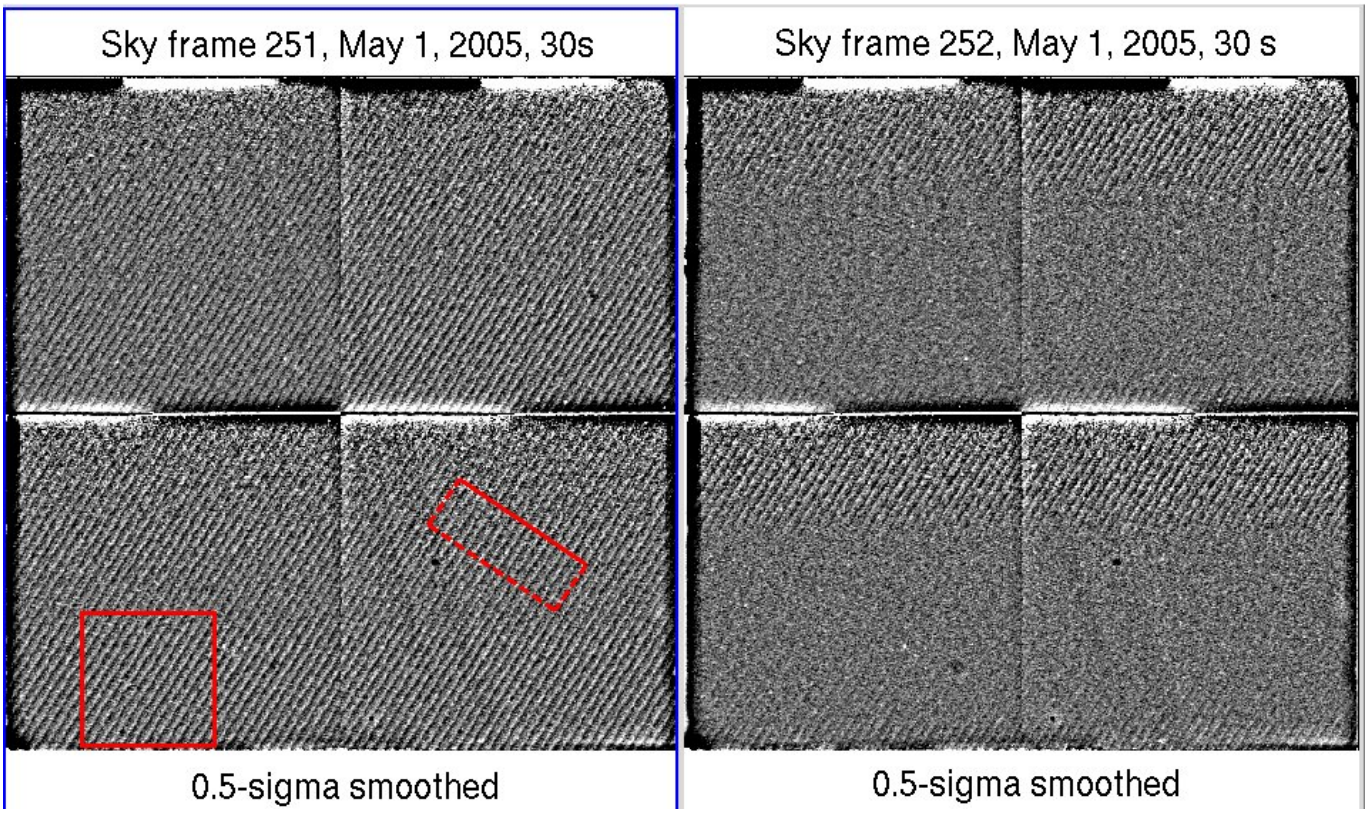

Figure 1: Two consecutive 30 s sky frames (after standard data processing) from the night of May 1, 2005. While the first frame displays a coherent, sinusoidal noise component, that noise component largely vanishes in the second frame. The 200x200 pixel rectangular region in the lower left corner is used to calculate periodic noise and read noise strength (see text). The rectangular region in the lower right corner is used to calculate a 1-d projection along the periodic noise.

apparent to the eye. However, while the pattern is coherent across the frame in the first frame, it only appears in patches in the second frame. This may be the result of beating with another periodic noise component. An animated gif with this series of frames (and several following frames) is available at: http:coatlicue.as.arizona.edu$\tilde{}$billerSDI_dark_May1.gif

For the rest of this section, we focus solely on sky frame 251, which displays a coherent periodic noise pattern along the entire frame. This frame is characteristic of the maximum amplitude noise pattern observed during this run. While many frames have similar amplitude noise patterns, some frames taken during this period also have lower noise amplitudes. (See the next section.)

In order to determine periodic noise properties, a 1-d projection along the periodic noise was calculated from the region depicted in Fig. 1. This projection is shown in Fig. 2. From the projection, we find a noise wavelength of 5.7 pixels and a peak-to-trough amplitude of 8 counts.

To disentangle read noise from the periodic noise and determine the relative strength of each component, we smoothed the standard-processed images (processed up to step

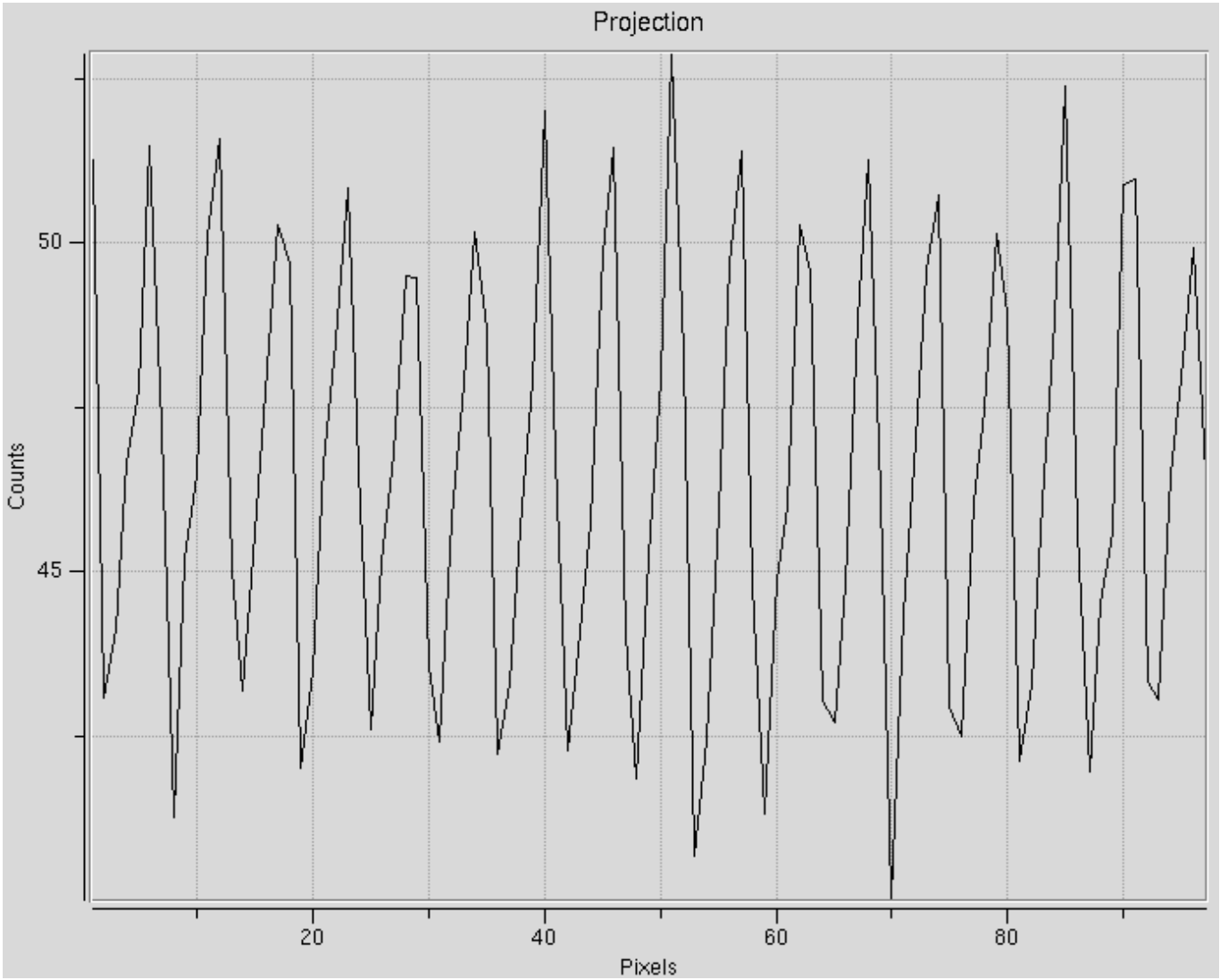

Figure 2: 1-d projection along the observed periodic noise. From the projection, we find a noise wavelength of 5.7 pixels and a peak-to-trough amplitude of 8 counts.

Image	Noise (counts)
0.5σ periodic	4.534
0.5σ read	2.99
1σ periodic	2.013
1σ read	4.466

5) by 0.5σ and 1σ gaussians. Each smoothed image was subtracted from the original image, removing the periodic noise. Only the high-frequency (varying on a pixel to pixel basis with no smooth component) read noise should remain in the the resulting images. Gaussian smoothed periodic noise images and read noise images are presented in Fig. 3.

The standard deviation within the 200x200 pixel box shown in Fig. 3 was calculated for each periodic noise image and each read noise image. These standard deviations are presented in Tab. 2.2. Unfortunately, we cannot entirely disentangle the read noise from the periodic noise. The 1σ smoothed read noise image still contains some periodic noise, while the 0.5σ smoothed periodic noise image still contains some pixel-to-pixel read noise. Using our noise estimates to calculate the relative strength of the periodic noise to the read noise, we find an upper limit of 1.5 times the read noise (ratio of 0.5σ periodic noise to read noise) and a lower limit of 0.45 times the read noise (ratio of 1σ periodic noise to read noise.) At any rate, the periodic noise is of the same order of magnitude as the read noise and is clearly visible above the read noise.

2.3 Noise Properties over Hour and Night Timescales

In order to determine how the noise amplitude varies over an hour-to-hour timescale, we calculated the standard deviation within a 200x200 pixel box (always the same box, which is shown in Fig. 3) for each sky frame 0.5σ smoothed periodic noise image from the night of May 1-2 2005. Standard deviations are plotted as a function of UT in Fig. 4. The noise amplitude increased by a factor of 1.6 from the beginning of the night (4 hrs UT) to the middle of the night (8 hrs UT).

2.4 Noise Properties over Several Observing Epochs

To characterize the noise properties over several epochs of ARIES SDI imaging, we chose example images to analyze from each epoch. Images were chosen with as obvious periodic noise properties as possible, so again, these are upper limits on the periodic noise. Other frames observed within the same epoch sometimes displayed smaller noise characteristics.

We estimate the wavelength and amplitude of the periodic noise (in Tab. 2.4) from 1-d projections calculated along the principle periodic noise component. 1-d projections for each of the images in Fig. 5 are displayed in Fig. 6. The rectangular regions used to calculate the projections are shown in Fig. 5.

In the October 2003, the periodic noise is rather obscured by the read-noise – amplitude and wavelength for this epoch are estimated from the coherent periodic patch between 10-20 pixels in the projection for this epoch. In February 2004, the periodic noise is visible but faint – similar in magnitude to the read noise. However, the amplitude of the periodic

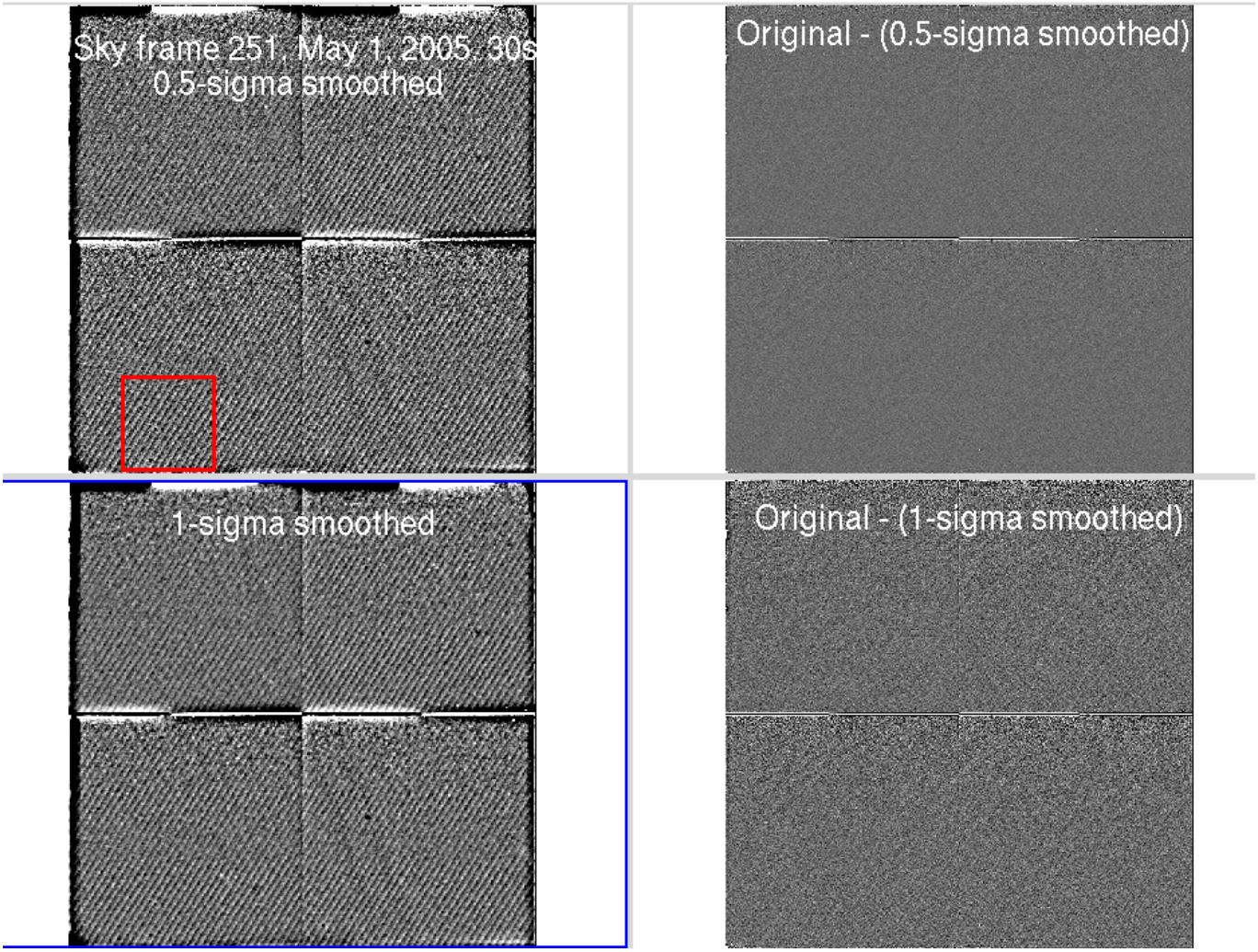

Figure 3: The standard processed image smoothed by a 1σ and 0.5σ gaussian are shown in the top left and bottom left image respectively. Read noise images produced from subtracting the smoothed periodic noise images from the original images are shown in the upper right (0.5σ smoothed) and lower right (1.0σ smoothed).

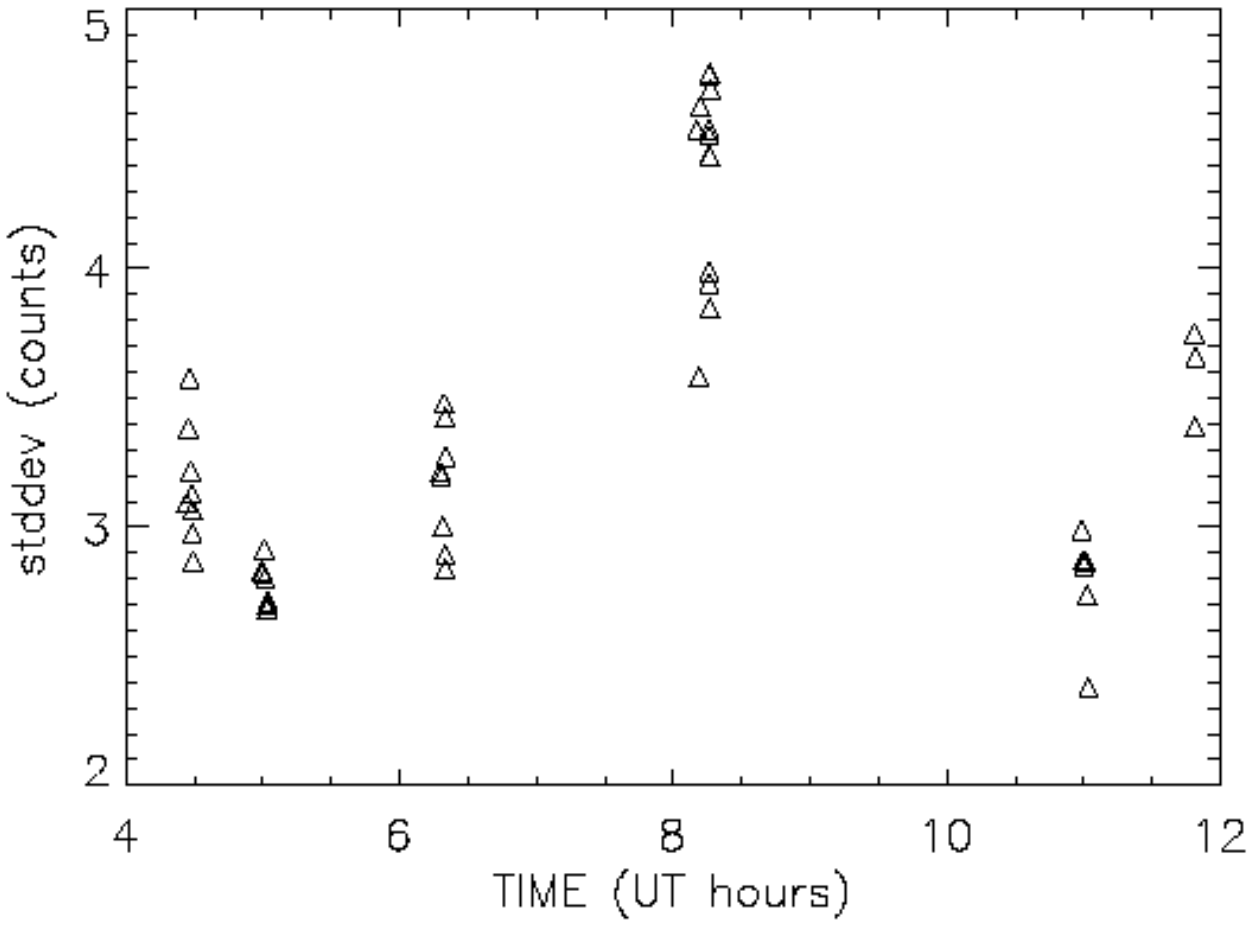

Figure 4: Standard deviation within a 200x200 pixel box is plotted vs. UT during the night of May 1-2, 2005. The noise amplitude increases by a factor of 1.6 between the beginning of the night (4 hrs UT) to the middle of the night (8 hrs UT)

Epoch	Amplitude (counts, peak to trough)	Wavelength (pixels)
May 2005	8	5.7
May 2004	3.3	2.3
Feb 2004	1	4
Oct 2003	2	2.5

noise appears to be growing over time and is certainly non-negligible in both the May 2004 and May 2005 images.

In general, the periodic noise component is detected with significantly higher confidence at later epochs compared to earlier epochs. Additionally, the wavelength of the periodic noise appears to be increasing with time. This suggests that we may be underestimating this noise component at earlier epochs where the spatial frequency of the noise is too high to be Nyquist sampled on our detector. Unfortunately, the spatial frequency of the noise at all epochs is similar to the spatial frequency at which one would expect to find planets. It is not inconceivable that a planet may fall on a peak in one image and in a trough in another, effectively preventing detection once several images are median-combined.

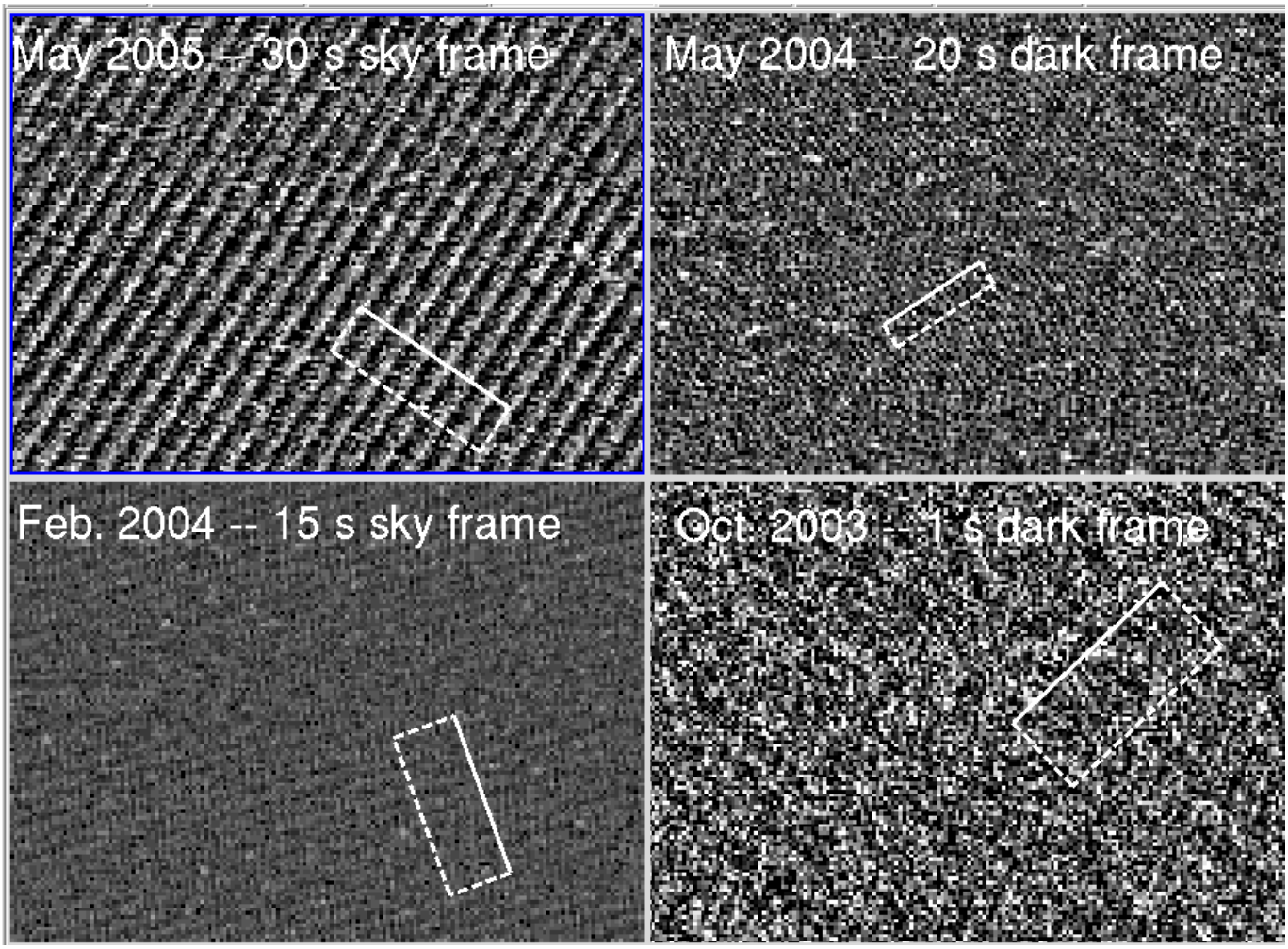

Figure 5: A representative noise image from each epoch of observation is shown. No smoothing has been performed on these images, so they may be regarded as the sum of the periodic noise component and the read noise component. The periodic noise component is clearly visible and dominates over the read noise in each image except the October 2003 image. The rectangular regions in each image are used to calculate 1-d projections along the periodic noise (presented in Fig. 6.

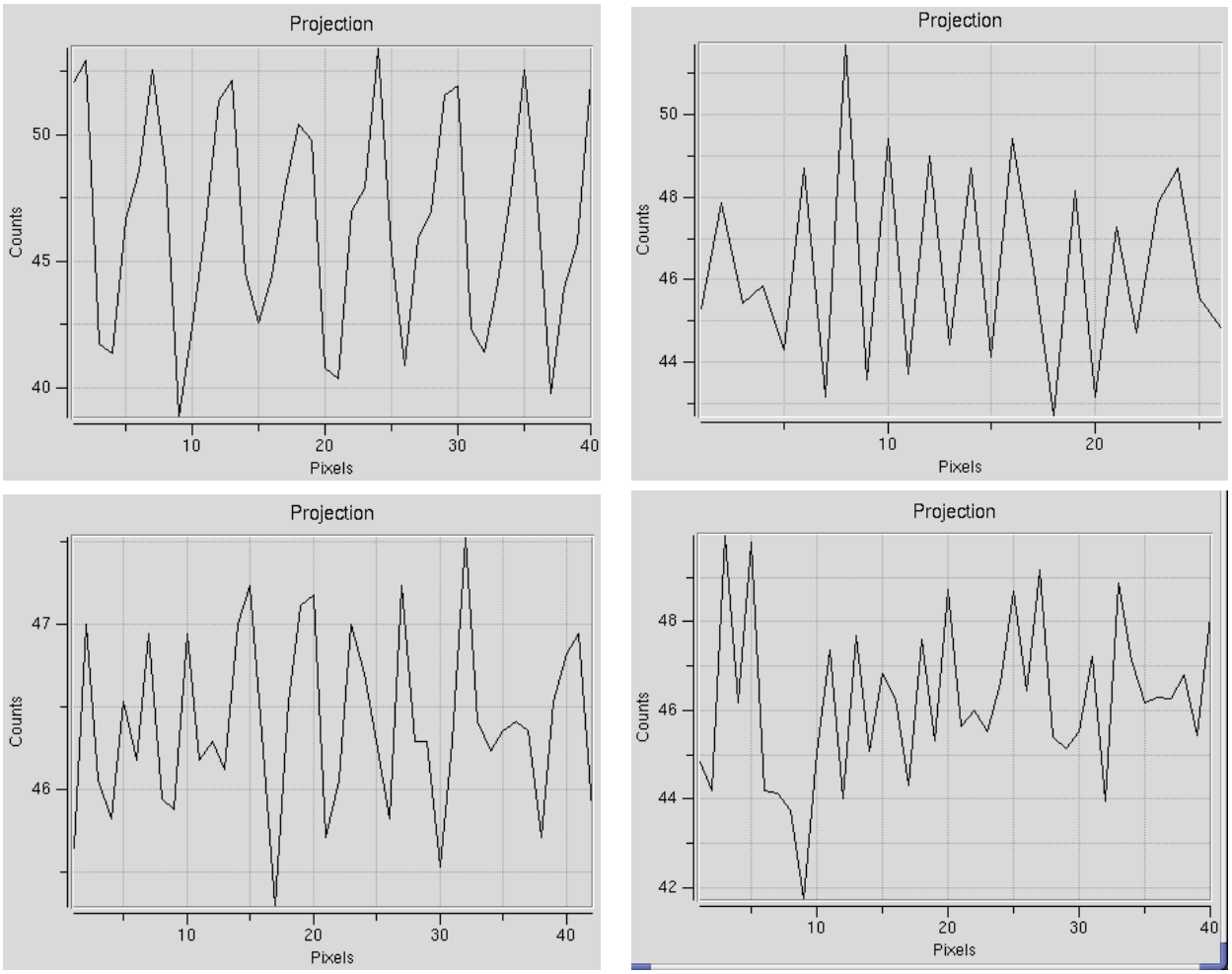

Figure 6: 1-d projections along the principle periodic noise component from each observing epoch. The May 2005 projection appears in the upper left corner, the May 2004 projection appears in the upper right corner, the Feb. 2004 projection appears in the lower left corner, and the October 2004 projection appears in the lower right corner.